



# HHS Public Access

Author manuscript

*Biochimie*. Author manuscript; available in PMC 2016 July 01.

Published in final edited form as:

*Biochimie*. 2015 July ; 114: 30–38. doi:10.1016/j.biochi.2015.04.001.

## The emerging role of rectified thermal fluctuations in initiator aa-tRNA- and start codon selection during translation initiation

Kelvin Caban and Ruben L. Gonzalez Jr.<sup>1</sup>

Department of Chemistry, Columbia University, New York, NY 10027

### Abstract

Decades of genetic, biochemical, biophysical, and structural studies suggest that the conformational dynamics of the translation machinery (TM), of which the ribosome is the central component, play a fundamental role in the mechanism and regulation of translation. More recently, single-molecule fluorescence resonance energy transfer (smFRET) studies have provided a unique and powerful approach for directly monitoring the real-time dynamics of the TM. Indeed, smFRET studies of the elongation stage of translation have significantly enriched our understanding of the mechanisms through which stochastic, thermally driven conformational fluctuations of the TM are exploited to drive and regulate the individual steps of translation elongation<sup>1</sup>. Beyond translation elongation, smFRET studies of the conformational dynamics of the initiation stage of translation offer great potential for providing mechanistic information that has thus far remained difficult or impossible to obtain using traditional methods. This is particularly true of the mechanisms through which the accuracy of initiator tRNA- and start codon selection is established during translation initiation. Given that translation initiation is a major checkpoint for regulating the translation of mRNAs, obtaining such mechanistic information holds great promise for our understanding of the translational regulation of gene expression. Here, we provide an overview of the bacterial translation initiation pathway, summarize what is known regarding the biochemical functions of the IFs, and discuss various new and exciting mechanistic insights that have emerged from several recently published smFRET studies of the mechanisms that guide initiator tRNA- and start codon selection during translation initiation. These studies provide a springboard for future investigations of the conformational dynamics of the more complex eukaryotic translation initiation pathway and mechanistic studies of the role of translational regulation of gene expression in human health and disease.

### Keywords

Translation initiation; ribosome; initiator tRNA; initiation factors; smFRET

### 1. Introduction

Synthesis of proteins via the translation of messenger RNAs (mRNAs) is universally catalyzed by the ribosome, a massive ( 2.5 MDa) two-subunit ribonucleoprotein molecular machine that comprises the central component of the cellular translation machinery (TM).

<sup>1</sup>To whom correspondence should be addressed: rlg2118@columbia.edu.

Over the past decade, single-molecule fluorescence energy transfer (smFRET) studies of the elongation stage of protein synthesis<sup>2-10</sup> have led to the view that the TM largely operates as a Brownian machine during translation elongation<sup>1,11</sup>. A Brownian machine is one that functions through stochastic, thermally driven conformational fluctuations that are systematically biased, or rectified, by the binding of a substrate, cofactor, or allosteric effector to the machine; execution of an irreversible chemical reaction by the machine; and/or release or diffusion of a reaction product from the machine<sup>12</sup>. Consistent with this functional framework, smFRET studies of translation elongation have revealed that many of the structural elements of the ribosome that have been implicated in driving translation elongation undergo thermal fluctuations that are rectified by the transfer RNA (tRNA) adaptors<sup>9</sup> and translation elongation factors (EFs) that interact with the ribosome during translation elongation<sup>4-8</sup>.

An example of the type of mechanistic insights that smFRET studies of translation elongation have provided come from investigations of the mechanisms that ensure the accuracy with which the TM selects the correct, mRNA-encoded aminoacyl-tRNA (aa-tRNA) during the aa-tRNA selection step of translation elongation<sup>3</sup>. Collectively, these studies have shown that, if delivery of an aa-tRNA to the ribosome results in the formation of a correctly base-paired mRNA codon-aa-tRNA anticodon interaction within the ribosomal aa-tRNA binding (A) site, the TM will rectify the thermal fluctuations of that aa-tRNA so as to favor its incorporation into the A site. Failure of an aa-tRNA to form a correctly base-paired codon-anticodon interaction at the A site, on the other hand, results in rectified fluctuations that promote the dissociation of that aa-tRNA from the A site.

It is notable that much less is known regarding the roles that rectified thermal fluctuations of the TM may play during translation initiation. Translation initiation involves the initiation factor (IF)-guided assembly of an intermediate ribosomal initiation complex (IC) at the start codon of the mRNA, and the subsequent conversion of this intermediate IC into one that is competent to enter the elongation stage of translation<sup>13</sup>. Comparative analysis of the structures of free translation initiation components and their structures within the context of a variety of ribosomal ICs, suggest that structural rearrangements might play a role in the mechanism and regulation of translation initiation<sup>14-19</sup>. Indeed, decades of biochemical studies of the translation initiation reaction have been interpreted within a framework that includes hypothesized conformational changes of initiation components<sup>13,20</sup>. Nonetheless, data directly demonstrating that these conformational changes indeed occur during translation initiation, the stage in the process in which they occur, and how they contribute to the mechanism remain elusive. Most importantly, due to the lack of structures of ribosomal ICs containing incorrect substrates, there is no information on the role that these dynamics might play in regulating the fidelity of translation initiation.

We begin this mini-review article by providing an overview of the bacterial translation initiation pathway and then reviewing what is known regarding the biochemical functions of the essential IFs. Subsequently, we discuss gaps in our understanding of how the IFs carry out their biochemical functions and how the results of recent smFRET studies, which have begun to reveal and characterize thermal fluctuations and associated rectifying mechanisms, have begun to address these gaps. Finally, we conclude by outlining what we think are some

of the most important remaining questions for future studies of the structural dynamics of both bacterial and eukaryotic translation initiation.

## 2. Overview of the bacterial translation initiation pathway

In bacteria, translation initiation proceeds through a highly dynamic, multi-step assembly pathway that leads to the formation of an elongation-competent 70S IC at the start codon of the mRNA (Fig. 1). 70S IC formation begins with the assembly of an intermediate 30S IC comprised of the small (30S) subunit, three essential IFs (IF1, the guanosine triphosphatase IF2, and IF3), mRNA, a specialized initiator tRNA (N-formyl-methionyl-tRNA<sup>fMet</sup> or fMet-tRNA<sup>fMet</sup>), and GTP. Subsequently, the large (50S) subunit joins to the 30S IC, giving rise to the 70S IC. During assembly of the 30S IC, two essential events must take place prior to the arrival of the 50S subunit. First, the 30S IC must select fMet-tRNA<sup>fMet</sup> from the cellular tRNA pool, which includes unaminoacylated and/or unformylated tRNA<sup>fMet</sup> as well as competing unaminoacylated and aminoacylated elongator tRNAs. Second, the 30S IC must select the correct start codon (AUG, CUG, or UUG, in bacteria) while discriminating against all non-start codons. Accurate fMet-tRNA<sup>fMet</sup> selection is an important event during translation initiation because it ensures that all of the proteins synthesized *in vivo* begin with formyl-methionine and thus have a correct N-terminus. Accurate start codon selection is perhaps even more important, as it establishes the reading frame of the mRNA, thereby ensuring that the correct sequence of codons is translated during translation elongation.

## 3. Accurate fMet-tRNA<sup>fMet</sup> and start codon selection is ensured by the opposing activities of IF2 and IF3

In bacteria, the vast majority of mRNAs contain a translation initiation region (TIR), which is composed of a consensus ribosome binding site referred to as the Shine-Dalgarno (SD) sequence, a downstream start codon, and a relatively short spacer sequence separating the SD sequence from the start codon. During translation initiation, selection of the start codon is facilitated by a base-pairing interaction between the SD sequence and the complementary anti-SD sequence on the 3' end of the 16S ribosomal RNA (rRNA) component of the 30S subunit<sup>21,22</sup>. The SD/anti-SD interaction physically localizes the start codon near the 30S peptidyl-tRNA binding (P)-site, making it accessible for base pairing with the fMet-tRNA<sup>fMet</sup> anticodon. In the absence of IFs, however, elongator aa-tRNAs compete efficiently with fMet-tRNA<sup>fMet</sup> for access to the P site<sup>23</sup>. As a result, non-start codons that are proximal to the start codon can be efficiently and incorrectly selected by establishing base-pairing interactions with their cognate elongator aa-tRNAs. When present simultaneously, on the other hand, the IFs collaborate to significantly reduce the likelihood that an elongator aa-tRNA and/or a non-start codon are selected at the P site, thereby greatly decreasing the probability of mis-initiation. The IFs achieve this by increasing the rate of association and decreasing the rate of dissociation of fMet-tRNA<sup>fMet</sup> relative to competing elongator aa-tRNAs<sup>24</sup>. Beyond their role in ensuring the accuracy of 30S IC assembly, the IFs also collaborate to couple the rate of 50S subunit joining to the composition of the 30S IC, thereby increasing the rate of subunit joining to correctly assembled 30S ICs while decreasing the rate of subunit joining to 'pseudo' 30S ICs carrying an unaminoacylated

tRNA<sup>fMet</sup>, unformylated Met-tRNA<sup>fMet</sup>, or an elongator aa-tRNA in the P site<sup>24</sup>, and ‘non-canonical’ 30S ICs assembled at a near-start codon<sup>25–27</sup>.

The collaborative effect of the IFs on the fidelity of translation initiation described above is primarily mediated by the opposing biochemical activities of IF2 and IF3. IF2 *positively* regulates the initiation reaction by selectively accelerating the rate of fMet-tRNA<sup>fMet</sup> association to the 30S IC over that of unaminoacylated and/or unformylated Met-tRNA<sup>fMet</sup> or elongator aa-tRNAs<sup>23,24</sup>. In addition, IF2 selectively accelerates the rate of 50S subunit joining to 30S ICs carrying a P site-bound fMet-tRNA<sup>fMet</sup> that is base-paired to a start codon<sup>24,28,29</sup>. In contrast, IF3 *negatively* regulates the initiation reaction by uniformly increasing the dissociation of all tRNAs, including fMet-tRNA<sup>fMet</sup>, from the P site of the 30S IC<sup>24</sup>. In addition, IF3 has subunit anti-association activity, which enables it to prevent the premature joining of the 50S subunit to 30S ICs lacking a tRNA at the P site<sup>28,30</sup>. IF3 also selectively inhibits subunit joining to pseudo 30S ICs<sup>24</sup> as well as 30S ICs assembled on mRNAs with suboptimal translation initiation regions<sup>26</sup>. Perhaps the most well established function of IF3, however, is its ability to selectively repress the translation of mRNAs that initiate with near-start codons<sup>25,31–37</sup>. IF3 exploits this latter function to autoregulate the translation of its own mRNA, which initiates with the near-start AUU codon<sup>38,39</sup>. IF3 discriminates against initiation at near-start codons, in part, by inhibiting subunit joining<sup>25,26</sup>.

#### 4. 30S IC-driven changes in the stability and dynamics of IF2 regulate initiator tRNA- and start codon selection

Despite our understanding of the biochemical functions of the IFs outlined in the previous section, the molecular mechanisms and structural bases through which the IFs exert these functions remain poorly defined. For example, although it is clear that IF2 primarily recognizes the formyl moiety of fMet-tRNA<sup>fMet</sup> and selectively accelerates the rate of 50S subunit joining to 30S ICs carrying a P site-bound fMet-tRNA<sup>fMet</sup> that is base-paired to a start codon, the molecular and structural events that are triggered by recognition of the formyl moiety of fMet-tRNA<sup>fMet</sup> by IF2 and that result in the observed acceleration of subunit joining remain unclear<sup>24</sup>. To address this gap in our understanding, several groups have recently generated cryogenic electron microscopy (cryo-EM)-based structural models of 30S ICs carrying a P site-bound fMet-tRNA<sup>fMet</sup> that is base paired to a start codon<sup>16,40</sup>. These structures have revealed that IF2 and fMet-tRNA<sup>fMet</sup> interact to form an IF2•tRNA sub-complex on the intersubunit surface of the 30S IC. Intriguingly, the position of the IF2•tRNA sub-complex on the 30S IC in these structures is such that it exhibits excellent shape complementarity to a large groove on the intersubunit surface of the 50S subunit<sup>41</sup>. These structures have therefore led to the proposal that IF2 primarily accelerates 50S subunit joining by making extensive interactions with its complementary groove in the 50S subunit and by permitting the formation of critical intersubunit bridge interactions between the 30S and 50S subunits<sup>41</sup>. Thus, it is possible that tRNA- and codon-dependent changes in the conformational dynamics of the IF2•tRNA sub-complex might provide the mechanistic and structural basis for coupling the rate of subunit joining to the tRNA-, and codon composition of the 30S IC. Nonetheless, the lack of structures of 30S ICs carrying unaminoacylated

and/or unformylated tRNA<sup>fMet</sup> or elongator tRNAs and/or non-start codons has thus far precluded testing and further development of this hypothesis.

To directly test the hypothesis that the conformational dynamics of the IF2•tRNA sub-complex depend on the identities of the P site-bound tRNA and codon, Wang *et al.* used a cyanine 5 (Cy5) FRET acceptor-labeled IF2 and cyanine 3 (Cy3) FRET donor-labeled tRNAs to develop an smFRET signal that enabled them to characterize the conformational dynamics of the IF2•tRNA sub-complex across a series of 30S ICs<sup>42</sup>. Highlighting the relatively complex compositional dynamics of translation initiation, individual 30S ICs in all of the 30S IC samples that were studied exhibited multiple cycles of IF2 binding and dissociation during the experimental observation time. Interestingly, the stability of IF2 binding to the 30S IC was found to be extraordinarily sensitive to the identity of the P site-bound tRNA, with pseudo 30S ICs carrying an unformylated Met-tRNA<sup>fMet</sup> or elongator Phe-tRNA<sup>Phe</sup> exhibiting 2–3 orders of magnitude lower affinity for IF2 than analogous canonical 30S ICs carrying a fMet-tRNA<sup>fMet</sup> (Fig. 2a). Beyond the affinity differences, the conformational dynamics of the IF2 and tRNA components of the IF2•tRNA sub-complexes that are formed within pseudo 30S ICs were significantly different than those within canonical 30S ICs. In the case of pseudo 30S ICs, the FRET efficiency (EFRET) versus time trajectories sampled EFRET values that were broadly distributed across the entire range of accessible values. In contrast, the EFRET trajectories of 30S ICs carrying an fMet-tRNA<sup>fMet</sup> exhibited EFRET values that were narrowly distributed and centered either at a single value or that fluctuated between two values. These results suggest that, depending on the identity of the P site-bound tRNA, IF2-bound 30S ICs will preferentially populate one of at least two thermally-accessible conformational states: a conformational state in which the IF2 and tRNA components of the IF2•tRNA sub-complex can adopt a relatively well-defined thermodynamically stable conformation(s) and IF2 is bound with a relatively high affinity or a conformational state in which they cannot adopt such conformation(s) and IF2 is bound with a relatively low affinity. Notably, 30S ICs analogous to those that preferentially sample the former conformational state have been shown to undergo relatively rapid subunit joining whereas pseudo 30S ICs analogous to those that preferentially sample the latter conformational state have been shown to undergo relatively slow subunit joining<sup>24</sup>. This strongly suggests that tRNA-dependent changes in the stability and dynamics of the IF2•tRNA sub-complex provides a means for coupling the rate of subunit joining to the tRNA composition of the 30S IC.

Similar results to those described for pseudo 30S ICs were obtained in analogous smFRET studies of non-canonical 30S ICs assembled at an AUU near-start codon relative to canonical 30S ICs assembled at an AUG start codon. In this case, however, the presence of IF1 and IF3 was required in order for the IF2-bound non-canonical 30S IC to adopt a conformational state in which IF2 is bound with an affinity that is 2 orders of magnitude lower relative to the analogous canonical 30S IC. This is consistent with previous biochemical data demonstrating that IF3 plays a key role in start-codon recognition<sup>25,31–37</sup> and, together with IF1, is required for coupling the rate of subunit joining to the codon composition of the 30S IC<sup>26,27</sup>. Although the IF1- and IF3-bound non-canonical 30S IC exhibited a significantly decreased affinity for IF2 relative to what is observed for the

analogous canonical 30S IC, the IF2•tRNA sub-complex did not exhibit significant differences in the distribution of EFRET values that were sampled. However, despite sampling similar EFRET values, the IF2•tRNA sub-complex within the IF1- and IF3-bound non-canonical 30S IC exhibited a substantial decrease in the conformational fluctuations among the non-zero EFRET values sampled relative to the analogous canonical 30S IC (Fig. 2b). Collectively, these observations indicate that the mechanism through which the rate of subunit joining is coupled to the codon composition of the 30S IC is different than the mechanism through which it is coupled to the tRNA composition of the 30S IC (*i.e.*, it is likely that IF1- and IF3-dependent conformational changes of the 30S IC beyond the relative positioning of the IF2•tRNA sub-complex also contribute to regulating the rate of subunit joining). Future cryo-EM and/or X-ray crystallographic structures of analogous pseudo and non-canonical 30S ICs should prove invaluable in helping to identify the various structural elements that couple the tRNA and codon composition of the 30S IC to the rate of 50S subunit joining. These structural studies will subsequently guide the development of additional smFRET signals to further characterize the dynamics of these conformationally flexible structural elements within the 30S IC.

## 5. The conformation of 30S IC-bound IF3 signals proper fMet-tRNA<sup>fMet</sup> and start codon selection

Kinetic studies have shown that IF3 binds rapidly and tightly to the 30S subunit suggesting that it is the first IF to associate with the 30S subunit *in vivo*<sup>43</sup>. At this early stage, IF3 promotes the dissociation of deacylated tRNAs from the P site of 30S subunits recycled from post termination complexes, thereby shuttling 30S subunits into the initiation pathway<sup>44</sup>. Furthermore, as noted above in Section 3, the presence of IF3 on the 30S subunit prevents premature joining of the 50S subunit to 30S ICs lacking a tRNA at the P site, which would otherwise result in the formation of a translationally inactive pool of 70S ribosomes<sup>28,30</sup>. Finally, 30S-bound IF3 increases the affinity of IF1 and IF2 for the 30S subunit thus ensuring that, given their cellular concentrations, 30S subunits would be saturated with all three IFs<sup>45-51</sup>.

Structurally, IF3 is comprised of globular N- and C-terminal domains that are separated by a flexible linker<sup>52</sup>. IF3 binds to the platform region of the 30S subunit in close proximity to the P site and the ribosomal tRNA exit (E) site<sup>16,53-56</sup>. Based on its location it has been suggested that IF3 blocks subunit joining by sterically occluding the formation of intersubunit bridges B2b and, possibly, B2c and B7a<sup>53,55</sup>. Although bacterial 70S ribosomes are held together by 12 independent intersubunit bridges, modification interference experiments have shown that interfering with the nucleotides involved in a subset of these bridges, including bridge B2b and B7a, is sufficient to disrupt stable subunit joining<sup>57</sup>.

Although IF3 blocks subunit joining in the early stages of the translation initiation pathway, its anti-association activity must somehow be alleviated upon formation of a completely and correctly assembled 30S IC (*i.e.*, a 30S IC carrying all three IFs and an fMet-tRNA<sup>fMet</sup> at an AUG start codon) so as to allow the initiation reaction to proceed. To address this conundrum, Ehrenberg and co-workers have proposed that the rate of spontaneous dissociation of IF3 from the 30S IC is accelerated upon formation of a completely and



correctly assembled 30S IC, thereby accelerating the rate of subunit joining<sup>28</sup>. Conflicting with this proposal, it was subsequently shown that the rate of 50S subunit joining to a completely and correctly formed 30S IC is slightly faster than the rate of IF3 dissociation, indicating that IF3 is released during subunit joining as the intersubunit bridges are being formed<sup>26</sup>. As an alternative model to that proposed by Ehrenberg and co-workers, it is possible that a completely and correctly formed 30S IC undergoes a conformational change that permits rapid 50S subunit joining despite the continued presence of IF3 within the 30S IC, a proposal that is supported by accumulating evidence that IF3<sup>43,56</sup> and the 30S subunit<sup>16,53–55,58</sup> can both undergo conformational changes when they interact.

Recently, Elvekrog and Gonzalez provided direct experimental evidence in support of this latter model by using smFRET to monitor the conformational dynamics of a 30S IC-bound IF3 variant in which the N- and C-terminal domains of the factor had been labeled with Cy3 and Cy5, respectively<sup>59</sup>. 30S IC-bound IF3 was observed to thermally fluctuate between at least three conformational states characterized by low-, intermediate-, and high EFRET values, suggesting that 30S IC-bound IF3 exists in a dynamic conformational equilibrium (Fig 3). Based on their EFRET values, these three conformational states of 30S IC-bound IF3 were designated as extended (low EFRET), intermediate (intermediate EFRET) and compact (high EFRET) conformations of IF3, respectively. Within the context of a 30S IC carrying all three IFs, but lacking fMet-tRNA<sup>fMet</sup>, IF3 predominantly occupies the extended conformation (Fig. 3a). Because 30S ICs lacking fMet-tRNA<sup>fMet</sup> are unable to undergo subunit joining, it is likely that the extended conformation of the 30S IC-bound IF3 represents a conformation of the 30S IC in which access to the 30S-subunit components of one or more of the intersubunit bridges that are required for stable subunit joining are restricted. Remarkably, in the context of a completely and correctly assembled 30S IC, there is a dramatic shift in the conformational equilibrium of 30S IC-bound IF3 towards the compact conformation (Fig. 3b). The compact conformation of the 30S IC-bound IF3 is likely to reflect a conformation of the 30S IC in which the 30S-subunit components of the intersubunit bridges that are presumably blocked within 30S ICs carrying an IF3 that is in the extended conformation have now become accessible, thereby permitting relatively rapid 50S subunit joining to 30S ICs that are still carrying IF3. Notably, analogous smFRET experiments recorded on pseudo and non-canonical 30S ICs demonstrated that the 30S IC-bound IF3 preferentially occupies the intermediate or extended conformations, virtually excluding the compact conformation (Fig. 3c and d). This observation is consistent with a model in which the compact conformation of the 30S IC-bound IF3 is strongly favored only within the context of 30S ICs carrying a P site-bound fMet-tRNA<sup>fMet</sup> that is base-paired to a start codon, thereby suggesting that the compact conformation of 30S IC-bound IF3 signals proper fMet-tRNA<sup>fMet</sup>- and start codon selection.

## 6. 30S IC-bound IF3 renders the subunit joining reaction reversible and produces two classes of subunit joining events

Collectively, the studies described above in Sections 4 and 5 suggest that the 30S IC, or components of the 30S IC, can undergo thermal fluctuations that are rectified in a tRNA- and/or codon-dependent manner to favor conformations that are either permissive or

inhibitory to subunit joining. Recently, MacDougall and Gonzalez have developed a FRET signal between a 30S IC carrying a Cy3-labeled IF2 variant and a 50S subunit carrying a Cy5-labeled ribosomal protein L11 (L11) variant that lays the groundwork for directly testing this hypothesis<sup>60</sup>. Stopped-flow delivery of 50S subunits reconstituted with Cy5-labeled L11 to 30S ICs carrying Cy3-labeled IF2 resulted in EFRET versus time trajectories that report on the subunit joining reaction in real time. Because of its well-established role in inhibiting and regulating the subunit joining reaction, MacDougall and Gonzalez began by conducting IF2-L11 smFRET studies of subunit joining in the absence and presence of IF3. In the absence of IF3, 50S subunits underwent stable and irreversible joining to the 30S IC, yielding a 70S IC that is relatively stable with a relatively long average lifetime of 100 s prior to dissociation into its component 30S IC and 50S subunits (Fig. 4a). In contrast, when IF3 was included within the 30S IC, subunit joining became a reversible process and individual subunit joining events could be clustered into at least two distinct classes of 70S ICs: (i) a 70S IC that is relatively unstable with a relatively short average lifetime of ~0.8 s prior to dissociation into its component 30S IC and 50S subunits and (ii) a 70S IC that is of intermediate stability with an intermediate average lifetime of 10 s prior to dissociation into its component 30S IC and 50S subunits (Fig. 4b). Notably, the lifetimes of the relatively unstable and intermediate-stability classes of 70S ICs were strikingly different from that of the relatively stable class of 70S IC observed in the absence of IF3, strongly suggesting that the relatively unstable and intermediate-stability classes of 70S ICs both contain bound IF3. Moreover, the multiple 50S subunit joining events that were observed for individual 30S ICs in the presence of IF3 could switch between the relatively unstable or intermediate-stability classes of 70S ICs, even under conditions in which free IF3 was removed from the imaging buffer. The removal of free IF3 from the imaging buffer virtually eliminates the possibility that a free IF3 molecule from the imaging buffer can bind to a 30S IC from which a bound IF3 molecule has dissociated. The results of these experiments, therefore, strongly suggest that the switching between short- and intermediate-lifetime classes of 70S ICs that is observed for individual 30S ICs arises from thermal fluctuations of IF3-bound 30S ICs as opposed to arising from the compositional heterogeneity generated by the possible dissociation of IF3 from a subset of 30S ICs.

Previous ensemble subunit joining studies have shown that when the concentration of free IF3 exceeds the amount of IF3 necessary to completely saturate the 30S ICs, the rate of subunit joining approaches zero<sup>28</sup>. Interestingly, when high concentrations of free IF3 (~1  $\mu$ M) were included in the imaging buffer used in the smFRET experiments described in the previous paragraph, 50S subunit joining resulted in 70S ICs that almost exclusively occupied the relatively unstable class of 70S ICs (Fig. 4c). This observation suggests that high concentrations of free IF3 in solution can rectify the thermal fluctuations of IF3-bound 30S ICs so as to favor the conformation of the 30S IC that results in formation of the relatively unstable class of 70S ICs. Recent single-molecule studies of the double-stranded DNA-binding (dsDNA) protein Fis may offer clues as to how free IF3 in solution may modulate the conformation of the IF3-bound 30S IC. In the absence of free Fis in solution, Fis has been shown to bind very stably to dsDNA, rarely exhibiting spontaneous dissociation events. Remarkably, however, the presence of high concentrations of free Fis in solution results in the accelerated turnover and rapid exchange of dsDNA-bound Fis with



free Fis from solution. By analogy, MacDougall and Gonzalez posit that the presence of high concentrations of IF3 free in solution may facilitate the exchange of 30S-bound IF3 with free IF3 from solution, a process that could rectify the thermal fluctuations of IF3-bound 30S ICs so as to favor the conformation of the 30S IC that results in formation of the relatively unstable class of 70S ICs. This may occur if, for instance, 30S IC-bound IF3 is constantly “turned over” before it has time to adopt a conformation within the 30S IC that is permissive for 50S subunit joining (*i.e.*, the compact conformation of 30S IC-bound IF3 described in Section 5).

## 7. Conclusions and future perspectives

The results of the several recent smFRET studies that we have reviewed here have begun to uncover the roles that rectified thermal fluctuations of the TM may play in ensuring the accuracy of fMet-tRNA<sup>fMet</sup>- and start codon selection during translation initiation. These studies have revealed dynamic aspects of the mechanisms of fMet-tRNA<sup>fMet</sup>- and start codon selection that, despite hints as to their potential importance have thus far remained difficult or impossible to access using ensemble biochemical and biophysical approaches. The available smFRET studies that we have reviewed here have been predominantly restricted to the fidelity of the 70S IC formation step of the translation initiation pathway, focusing on the thermal fluctuations of several components of pre-assembled 30S ICs and how the rectification of these fluctuations might contribute to the mechanism through which the rate of 50S subunit joining is coupled to the tRNA- and codon composition of the 30S IC. A much greater challenge, however, will be to investigate the fidelity of the 30S IC formation step of translation initiation to elucidate the mechanisms through which fMet-tRNA<sup>fMet</sup> is accurately recruited and positioned, along with the start codon, into the P site. In a landmark experiment, Puglisi and co-workers used single-molecule nanoaperture fluorescence microscopy to determine the order in which fluorescently labeled fMet-tRNA<sup>fMet</sup> and IF2 are recruited to the 30S subunit during 30S IC assembly<sup>61</sup>. Highlighting the complex compositional dynamics of translation initiation, Puglisi and co-workers found that there is no defined order in which fMet-tRNA<sup>fMet</sup> and IF2 must be recruited to the 30S IC and that the order in which they are preferentially recruited depends on the concentrations of fMet-tRNA<sup>fMet</sup> and IF2 as well as on the absence or presence of IF1 and IF3 within the 30S IC. Extension of these experiments to include fluorescently labeled IF1 and IF3 as well as tRNAs other than fMet-tRNA<sup>fMet</sup> and non-start codons should ultimately allow elucidation of the mechanisms through which fMet-tRNA<sup>fMet</sup> and the start codon are specifically recruited and positioned into the P site during 30S IC assembly while simultaneously shedding light on how the incorrect substrates are selected against.

Additional breakthroughs in our understanding of the mechanism of translation initiation and its regulation will require the development of an expanded repertoire of smFRET signals for monitoring the dynamics of additional components of the 30S IC and 70S IC. Development of dual labeled IF2 variants, for example, should allow the intramolecular dynamics of 30S IC-bound IF2 during translation initiation to be characterized in a manner analogous to what has been done for IF3 (Section 5)<sup>59</sup>. Several biochemical<sup>62,63</sup> and structural<sup>15–19,40,41,64</sup> studies suggest that such intramolecular dynamics of IF2 may be important determinants for driving and regulating translation initiation and smFRET signals

that report on these dynamics may provide unique and powerful mechanistic insights into these processes. Similarly, numerous genetic<sup>27,36,65</sup>, biochemical<sup>25,26,29</sup>, and structural studies<sup>16,40,41,66</sup> suggest that, in addition to the 30S IC-bound IFs and tRNA, the 30S subunit itself undergoes structural rearrangements during the 30S IC- and 70S IC formation steps of translation initiation that may be functionally relevant and important. Like many of the other large-scale conformational changes that the TM undergoes during protein synthesis, it is likely that structural rearrangements of the 30S IC are thermally activated and rectified in ways that drive and regulate the 30S IC- and 70S IC formation steps of translation initiation. Consequently, a full mechanistic understanding of translation initiation will likely require smFRET studies of new smFRET signals that, using fluorescently labeled 30S subunits, report directly on the conformational dynamics of individual structural elements of the 30S subunit during translation initiation.

Yet another important and challenging future goal for the translation field is to extend the smFRET approaches for studying bacterial translation that have been developed over the past decade to studies of eukaryotic translation. Nowhere will the significance of such an accomplishment be higher than in studies of eukaryotic translation initiation. In eukaryotes, translation initiation is a major target for the post-transcriptional control of gene expression. The vast majority of translationally regulated genes, including many involved in development and differentiation, are regulated at the level of translation initiation<sup>67–69</sup>. As such, the initiation pathway is an exceptionally vulnerable target for numerous cellular pathogens<sup>70–75</sup>. In fact, deregulation of initiation is causally linked to tumorigenesis<sup>69,76–82</sup> and viral infections<sup>71,73–75</sup> in humans.

Befitting the expanded role of translational regulation in eukaryotes versus bacteria, the translation initiation pathway in eukaryotes is significantly more complex than that of bacteria. Although several features of the pathway are universal (*e.g.*, IF1, IF2, and IF3 all have sequence and/or functional homologs in eukaryotic cells, termed eIF1A, eIF5B, and eIF1, respectively)<sup>83</sup>, eukaryotes encode at least nine additional eukaryotic IFs (eIFs), incorporate eukaryotic-specific mRNA elements (*e.g.*, the 5' 7-methylguanosine “cap” and the 3' polyadenine “tail”), and have evolved additional steps in the initiation pathway (*e.g.*, scanning of the ribosome along the mRNA to locate the start codon and circularization of the mRNA) that enable additional, eukaryotic-specific opportunities to regulate translation initiation and, consequently, gene expression. As is the case with the bacterial initiation pathway, current models of the eukaryotic initiation pathway are replete with compositional and conformational intermediates that have been inferred from numerous genetic, biochemical and structural studies<sup>84</sup>. A prominent example is the “open” scanning-competent conformation of the small, 40S, ribosomal subunit observed when comparing the cryo-EM structures of the free 40S subunit and the 40S subunit bound to eIF1 and eIF1A<sup>85</sup>. smFRET studies have the power to interrogate such conformational changes in real-time, thereby allowing for the detailed kinetic and thermodynamic characterization of these dynamics and their regulation.

## Acknowledgments

We sincerely apologize to our many colleagues whose work we could not include or cite due to space limitations. In addition, we would like to thank Dr. Daniel MacDougall, Dr. Margaret Elvekrog, and Dr. Jiangning Wang for many insightful discussions. This work was supported by a Burroughs Wellcome Fund CABS Award (CABS 1004856), an NSF CAREER Award (MCB 0644262), an NIH-NIGMS grant (R01 GM084288), an American Cancer Society Research Scholar Grant (RSG GMC-117152), and a Camille Dreyfus Teacher-Scholar Award to R.L.G. K.C. was supported by an American Cancer Society Postdoctoral Fellowship (125201).

## References

1. Frank J, Gonzalez RL. Structure and dynamics of a processive Brownian motor: the translating ribosome. *Annu Rev Biochem.* 2010; 79:381–412. [PubMed: 20235828]
2. Blanchard SC, Kim HD, Gonzalez RL, Puglisi JD, Chu S. tRNA dynamics on the ribosome during translation. *Proc Natl Acad Sci U S A.* 2004; 101:12893–12898. [PubMed: 15317937]
3. Blanchard SC, Gonzalez RL, Kim HD, Chu S, Puglisi JD. tRNA selection and kinetic proofreading in translation. *Nat Struct Mol Biol.* 2004; 11:1008–1014. [PubMed: 15448679]
4. Fei J, Kosuri P, MacDougall DD, Gonzalez RL. Coupling of ribosomal L1 stalk and tRNA dynamics during translation elongation. *Mol Cell.* 2008; 30:348–359. [PubMed: 18471980]
5. Cornish PV, Ermolenko DN, Noller HF, Ha T. Spontaneous intersubunit rotation in single ribosomes. *Mol Cell.* 2008; 30:578–588. [PubMed: 18538656]
6. Marshall RA, Dorywalska M, Puglisi JD. Irreversible chemical steps control intersubunit dynamics during translation. *Proc Natl Acad Sci U S A.* 2008; 105:15364–15369. [PubMed: 18824686]
7. Cornish PV, Ermolenko DN, Staple DW, Hoang L, Hickerson RP, Noller HF, Ha T. Following movement of the L1 stalk between three functional states in single ribosomes. *Proc Natl Acad Sci U S A.* 2009; 106:2571–2576. [PubMed: 19190181]
8. Fei J, Bronson JE, Hofman JM, Srinivas RL, Wiggins CH, Gonzalez RL. Allosteric collaboration between elongation factor G and the ribosomal L1 stalk directs tRNA movements during translation. *Proc Natl Acad Sci U S A.* 2009; 106:15702–15707. [PubMed: 19717422]
9. Fei J, Richard AC, Bronson JE, Gonzalez RL. Transfer RNA-mediated regulation of ribosome dynamics during protein synthesis. *Nat Struct Mol Biol.* 2011; 18:1043–1051. [PubMed: 21857664]
10. Ning W, Fei J, Gonzalez RL. The ribosome uses cooperative conformational changes to maximize and regulate the efficiency of translation. *Proc Natl Acad Sci U S A.* 2014
11. Tinoco I, Gonzalez RL. Biological mechanisms, one molecule at a time. *Genes Dev.* 2011; 25:1205–1231. [PubMed: 21685361]
12. Astumian RD. Thermodynamics and kinetics of a Brownian motor. *Science.* 1997; 276:917–922. [PubMed: 9139648]
13. Laursen BS, Sørensen HP, Mortensen KK, Sperling-Petersen HU. Initiation of protein synthesis in bacteria. *Microbiol Mol Biol Rev.* 2005; 69:101–123. [PubMed: 15755955]
14. Simonetti A, Marzi S, Jenner L, Myasnikov A, Romby P, Yusupova G, Klaholz BP, Yusupov M. A structural view of translation initiation in bacteria. *Cell Mol Life Sci.* 2009; 66:423–436. [PubMed: 19011758]
15. Vohlander Rasmussen LC, Oliveira CL, Pedersen JS, Sperling-Petersen HU, Mortensen KK. Structural transitions of translation initiation factor IF2 upon GDPNP and GDP binding in solution. *Biochemistry.* 2011; 50:9779–9787. [PubMed: 21988058]
16. Julián P, Milon P, Agirrezabala X, Lasso G, Gil D, Rodnina MV, Valle M. The Cryo-EM structure of a complete 30S translation initiation complex from *Escherichia coli*. *PLoS Biol.* 2011; 9:e1001095. [PubMed: 21750663]
17. Wienk H, Tishchenko E, Belardinelli R, Tomaselli S, Dongre R, Spurio R, Folkers GE, Gualerzi CO, Boelens R. Structural dynamics of bacterial translation initiation factor IF2. *J Biol Chem.* 2012; 287:10922–10932. [PubMed: 22308033]
18. Simonetti A, Marzi S, Fabbretti A, Hazemann I, Jenner L, Urzhumtsev A, Gualerzi CO, Klaholz BP. Structure of the protein core of translation initiation factor 2 in apo, GTP-bound and GDP-bound forms. *Acta Crystallogr D Biol Crystallogr.* 2013; 69:925–933. [PubMed: 23695237]

19. Eiler D, Lin J, Simonetti A, Klaholz BP, Steitz TA. Initiation factor 2 crystal structure reveals a different domain organization from eukaryotic initiation factor 5B and mechanism among translational GTPases. *Proc Natl Acad Sci U S A*. 2013; 110:15662–15667. [PubMed: 24029018]
20. Milón P, Rodnina MV. Kinetic control of translation initiation in bacteria. *Crit Rev Biochem Mol Biol*. 2012; 47:334–348. [PubMed: 22515367]
21. Shine J, Dalgarno L. The 3'-terminal sequence of *Escherichia coli* 16S ribosomal RNA: complementarity to nonsense triplets and ribosome binding sites. *Proc Natl Acad Sci U S A*. 1974; 71:1342–1346. [PubMed: 4598299]
22. Steitz JA, Jakes K. How ribosomes select initiator regions in mRNA: base pair formation between the 3' terminus of 16S rRNA and the mRNA during initiation of protein synthesis in *Escherichia coli*. *Proc Natl Acad Sci U S A*. 1975; 72:4734–4738. [PubMed: 1107998]
23. Hartz D, McPheeters DS, Gold L. Selection of the initiator tRNA by *Escherichia coli* initiation factors. *Genes Dev*. 1989; 3:1899–1912. [PubMed: 2695390]
24. Antoun A, Pavlov MY, Lovmar M, Ehrenberg M. How initiation factors maximize the accuracy of tRNA selection in initiation of bacterial protein synthesis. *Mol Cell*. 2006; 23:183–193. [PubMed: 16857585]
25. Grigoriadou C, Marzi S, Pan D, Gualerzi CO, Cooperman BS. The translational fidelity function of IF3 during transition from the 30 S initiation complex to the 70 S initiation complex. *J Mol Biol*. 2007; 373:551–561. [PubMed: 17868695]
26. Milon P, Konevega AL, Gualerzi CO, Rodnina MV. Kinetic checkpoint at a late step in translation initiation. *Mol Cell*. 2008; 30:712–720. [PubMed: 18570874]
27. Qin D, Liu Q, Devaraj A, Fredrick K. Role of helix 44 of 16S rRNA in the fidelity of translation initiation. *RNA*. 2012; 18:485–495. [PubMed: 22279149]
28. Antoun A, Pavlov MY, Lovmar M, Ehrenberg M. How initiation factors tune the rate of initiation of protein synthesis in bacteria. *EMBO J*. 2006; 25:2539–2550. [PubMed: 16724118]
29. Grigoriadou C, Marzi S, Kirillov S, Gualerzi CO, Cooperman BS. A quantitative kinetic scheme for 70 S translation initiation complex formation. *J Mol Biol*. 2007; 373:562–572. [PubMed: 17868692]
30. Antoun A, Pavlov MY, Tenson T, Ehrenberg M. Ribosome formation from subunits studied by stopped-flow and Rayleigh light scattering. *Biol Proced Online*. 2004; 6:35–54. [PubMed: 15103398]
31. Sacerdot C, Chiaruttini C, Engst K, Graffe M, Milet M, Mathy N, Dondon J, Springer M. The role of the AUU initiation codon in the negative feedback regulation of the gene for translation initiation factor IF3 in *Escherichia coli*. *Mol Microbiol*. 1996; 21:331–346. [PubMed: 8858588]
32. Sussman JK, Simons EL, Simons RW. *Escherichia coli* translation initiation factor 3 discriminates the initiation codon in vivo. *Mol Microbiol*. 1996; 21:347–360. [PubMed: 8858589]
33. Haggerty TJ, Lovett ST. IF3-mediated suppression of a GUA initiation codon mutation in the *recJ* gene of *Escherichia coli*. *J Bacteriol*. 1997; 179:6705–6713. [PubMed: 9352920]
34. Sacerdot C, de Cock E, Engst K, Graffe M, Dardel F, Springer M. Mutations that alter initiation codon discrimination by *Escherichia coli* initiation factor IF3. *J Mol Biol*. 1999; 288:803–810. [PubMed: 10329180]
35. O'Connor M, Gregory ST, Rajbhandary UL, Dahlberg AE. Altered discrimination of start codons and initiator tRNAs by mutant initiation factor 3. *RNA*. 2001; 7:969–978. [PubMed: 11453069]
36. Qin D, Abdi NM, Fredrick K. Characterization of 16S rRNA mutations that decrease the fidelity of translation initiation. *RNA*. 2007; 13:2348–2355. [PubMed: 17942743]
37. Maar D, Liveris D, Sussman JK, Ringquist S, Moll I, Heredia N, Kil A, Bläsi U, Schwartz I, Simons RW. A single mutation in the IF3 N-terminal domain perturbs the fidelity of translation initiation at three levels. *J Mol Biol*. 2008; 383:937–944. [PubMed: 18805426]
38. Butler J, Springer M, Dondon J, Graffe M, Grunberg-Manago M. *Escherichia coli* protein synthesis initiation factor IF3 controls its own gene expression at the translational level in vivo. *Journal of Molecular Biology*. 1986; 192:767–780. [PubMed: 2438418]
39. Butler JS, Springer M, Grunberg-Manago M. AUU-to-AUG mutation in the initiator codon of the translation initiation factor IF3 abolishes translational autocontrol of its own gene (*infC*) in vivo. *Proc Natl Acad Sci U S A*. 1987; 84:4022–4025. [PubMed: 2954162]

40. Simonetti A, Marzi S, Myasnikov AG, Fabbretti A, Yusupov M, Gualerzi CO, Klaholz BP. Structure of the 30S translation initiation complex. *Nature*. 2008; 455:416–420. [PubMed: 18758445]
41. Allen GS, Zavialov A, Gursky R, Ehrenberg M, Frank J. The cryo-EM structure of a translation initiation complex from *Escherichia coli*. *Cell*. 2005; 121:703–712. [PubMed: 15935757]
42. Wang J, Caban K, Gonzalez RL. Ribosomal Initiation Complex-Driven Changes in the Stability and Dynamics of Initiation Factor 2 Regulate the Fidelity of Translation Initiation. *J Mol Biol*. 2015
43. Milón P, Maracci C, Filonava L, Gualerzi CO, Rodnina MV. Real-time assembly landscape of bacterial 30S translation initiation complex. *Nat Struct Mol Biol*. 2012; 19:609–615. [PubMed: 22562136]
44. Karimi R, Pavlov MY, Buckingham RH, Ehrenberg M. Novel Roles for Classical Factors at the Interface between Translation Termination and Initiation. *Molecular Cell*. 1999; 3:601–609. [PubMed: 10360176]
45. Howe JG, Yanov J, Meyer L, Johnston K, Hershey JW. Determination of protein synthesis initiation factor levels in crude lysates of *Escherichia coli* by a sensitive radioimmuno assay. *Archives of biochemistry and biophysics*. 1978; 191:813–820. [PubMed: 105669]
46. Weiel J, Hershey JW. Fluorescence polarization studies of the binding of fluorescein-labeled initiation factor IF3 to 30 S ribosomal subunits from *Escherichia coli*. *FEBS Lett*. 1978; 87:103–106. [PubMed: 344061]
47. Weiel J, Hershey JW. Fluorescence polarization studies of the interaction of *Escherichia coli* protein synthesis initiation factor 3 with 30S ribosomal subunits. *Biochemistry*. 1981; 20:5859–5865. [PubMed: 7028112]
48. Howe JG, Hershey JW. A sensitive immunoblotting method for measuring protein synthesis initiation factor levels in lysates of *Escherichia coli*. *J Biol Chem*. 1981; 256:12836–12839. [PubMed: 7031052]
49. Weiel J, Hershey JW. The binding of fluorescein-labeled protein synthesis initiation factor 2 to *Escherichia coli* 30 S ribosomal subunits determined by fluorescence polarization. *J Biol Chem*. 1982; 257:1215–1220. [PubMed: 6799502]
50. Howe JG, Hershey JW. Initiation factor and ribosome levels are coordinately controlled in *Escherichia coli* growing at different rates. *J Biol Chem*. 1983; 258:1954–1959. [PubMed: 6337147]
51. Zucker FH, Hershey JW. Binding of *Escherichia coli* protein synthesis initiation factor IF1 to 30S ribosomal subunits measured by fluorescence polarization. *Biochemistry*. 1986; 25:3682–3690. [PubMed: 3521729]
52. Moreau M, de Cock E, Fortier PL, Garcia C, Albaret C, Blanquet S, Lallemand JY, Dardel F. Heteronuclear NMR studies of *E. coli* translation initiation factor IF3. Evidence that the inter-domain region is disordered in solution. *J Mol Biol*. 1997; 266:15–22. [PubMed: 9054966]
53. Moazed D, Samaha RR, Gualerzi C, Noller HF. Specific protection of 16 S rRNA by translational initiation factors. *Journal of molecular biology*. 1995; 248:207–210. [PubMed: 7739034]
54. McCutcheon JP, Agrawal RK, Philips SM, Grassucci RA, Gerchman SE, Clemons WM, Ramakrishnan V, Frank J. Location of translational initiation factor IF3 on the small ribosomal subunit. *Proc Natl Acad Sci U S A*. 1999; 96:4301–4306. [PubMed: 10200257]
55. Dallas A, Noller HF. Interaction of translation initiation factor 3 with the 30S ribosomal subunit. *Molecular cell*. 2001; 8:855–864. [PubMed: 11684020]
56. Fabbretti A, Pon CL, Hennelly SP, Hill WE, Lodmell JS, Gualerzi CO. The real-time path of translation factor IF3 onto and off the ribosome. *Mol Cell*. 2007; 25:285–296. [PubMed: 17244535]
57. Pulk A, Maiväli U, Remme J. Identification of nucleotides in *E. coli* 16S rRNA essential for ribosome subunit association. *RNA*. 2006; 12:790–796. [PubMed: 16556933]
58. Paradies HH, Franz A, Pon CL, Gualerzi C. Conformational transition of the 30 S ribosomal subunit induced by initiation factor 3 (IF-3). *Biochem Biophys Res Commun*. 1974; 59:600–607. [PubMed: 4604265]



59. Elvekrog MM, Gonzalez RL. Conformational selection of translation initiation factor 3 signals proper substrate selection. *Nat Struct Mol Biol.* 2013; 20:628–633. [PubMed: 23584454]
60. MacDougall DD, Gonzalez RL. Translation initiation factor 3 regulates switching between different modes of ribosomal subunit joining. *Journal of molecular biology.* 2014
61. Tsai A, Petrov A, Marshall RA, Korlach J, Uemura S, Puglisi JD. Heterogeneous pathways and timing of factor departure during translation initiation. *Nature.* 2012; 487:390–393. [PubMed: 22722848]
62. Zorzet A, Pavlov MY, Nilsson AI, Ehrenberg M, Andersson DI. Error-prone initiation factor 2 mutations reduce the fitness cost of antibiotic resistance. *Mol Microbiol.* 2010; 75:1299–1313. [PubMed: 20132454]
63. Pavlov MY, Zorzet A, Andersson DI, Ehrenberg M. Activation of initiation factor 2 by ligands and mutations for rapid docking of ribosomal subunits. *EMBO J.* 2011; 30:289–301. [PubMed: 21151095]
64. Myasnikov AG, Marzi S, Simonetti A, Giuliodori AM, Gualerzi CO, Yusupova G, Yusupov M, Klaholz BP. Conformational transition of initiation factor 2 from the GTP- to GDP-bound state visualized on the ribosome. *Nat Struct Mol Biol.* 2005; 12:1145–1149. [PubMed: 16284619]
65. Qin D, Fredrick K. Control of translation initiation involves a factor-induced rearrangement of helix 44 of 16S ribosomal RNA. *Mol Microbiol.* 2009; 71:1239–1249. [PubMed: 19154330]
66. Carter AP, Clemons WM, Brodersen DE, Morgan-Warren RJ, Hartsch T, Wimberly BT, Ramakrishnan V. Crystal structure of an initiation factor bound to the 30S ribosomal subunit. *Science.* 2001; 291:498–501. [PubMed: 11228145]
67. Mathews MB, Sonenberg N, Hershey JWB. *Origins and Principles of Translational Control. Translational Control of Gene Expression.* 2000:1–31.
68. Sonenberg N, Dever TE. Eukaryotic translation initiation factors and regulators. *Curr Opin Struct Biol.* 2003; 13:56–63. [PubMed: 12581660]
69. Sonenberg N, Hinnebusch AG. New modes of translational control in development, behavior, and disease. *Mol Cell.* 2007; 28:721–729. [PubMed: 18082597]
70. Robertson ES, Nicholson AW. Phosphorylation of Escherichia coli translation initiation factors by the bacteriophage T7 protein kinase. *Biochemistry.* 1992; 31:4822–4827. [PubMed: 1534259]
71. Pe'ery, T.; Mathews, MB. *Viral Translation Strategies and Host Defense Mechanisms.* In: Sonenberg, N.; Hershey, JWB.; Mathews, M., editors. *Translational Control of Gene Expression.* Cold Spring Harbor Laboratory Press; Cold Spring Harbor: 2000. p. 371-424.
72. Miller ES, Kutter E, Mosig G, Arisaka F, Kunisawa T, R ger W. Bacteriophage T4 genome. *Microbiol Mol Biol Rev.* 2003; 67:86–156. table of contents. [PubMed: 12626685]
73. Schneider RJ, Mohr I. Translation initiation and viral tricks. *Trends Biochem Sci.* 2003; 28:130–136. [PubMed: 12633992]
74. Mohr I. Neutralizing innate host defenses to control viral translation in HSV-1 infected cells. *Int Rev Immunol.* 2004; 23:199–220. [PubMed: 14690861]
75. Walsh D, Mathews MB, Mohr I. Tinkering with translation: protein synthesis in virus-infected cells. *Cold Spring Harb Perspect Biol.* 2013; 5:a012351. [PubMed: 23209131]
76. Clemens MJ, Bommer UA. Translational control: the cancer connection. *Int J Biochem Cell Biol.* 1999; 31:1–23. [PubMed: 10216939]
77. Hershey, JWB.; Merrick, WC. *The Pathway and Mechanism of Initiation of Protein Synthesis.* In: Sonenberg, N.; Hershey, JWB.; Mathews, M., editors. *Translational Control of Gene Expression.* Cold Spring Harbor Laboratory Press; Cold Spring Harbor: 2000. p. 33-88.
78. Dua K, Williams TM, Beretta L. Translational control of the proteome: relevance to cancer. *Proteomics.* 2001; 1:1191–1199. [PubMed: 11721631]
79. Watkins SJ, Norbury CJ. Translation initiation and its deregulation during tumorigenesis. *Br J Cancer.* 2002; 86:1023–1027. [PubMed: 11953842]
80. Clemens MJ. Targets and mechanisms for the regulation of translation in malignant transformation. *Oncogene.* 2004; 23:3180–3188. [PubMed: 15094767]
81. De Benedetti A, Graff JR. eIF-4E expression and its role in malignancies and metastases. *Oncogene.* 2004; 23:3189–3199. [PubMed: 15094768]



82. Ruggero D. Translational control in cancer etiology. *Cold Spring Harb Perspect Biol.* 2013; 5
83. Allen GS, Frank J. Structural insights on the translation initiation complex: ghosts of a universal initiation complex. *Mol Microbiol.* 2007; 63:941–950. [PubMed: 17238926]
84. Hinnebusch AG, Lorsch JR. The mechanism of eukaryotic translation initiation: new insights and challenges. *Cold Spring Harb Perspect Biol.* 2012; 4
85. Passmore LA, Schmeing TM, Maag D, Applefield DJ, Acker MG, Algire MA, Lorsch JR, Ramakrishnan V. The eukaryotic translation initiation factors eIF1 and eIF1A induce an open conformation of the 40S ribosome. *Mol Cell.* 2007; 26:41–50. [PubMed: 17434125]

Author Manuscript

Author Manuscript

Author Manuscript

Author Manuscript

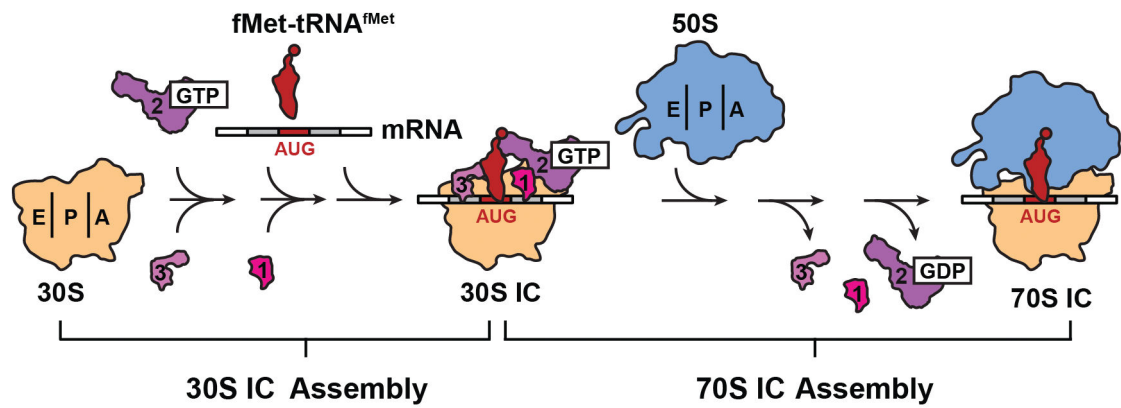


**Figure 1.**

Bacterial translation initiation pathway. The multi-step initiation pathway proceeds through the assembly of an intermediate 30S initiation complex (30S IC) comprised of the small, 30S ribosomal subunit, three initiation factors (IF1, 2 and 3), the messenger RNA (mRNA), and initiator fMet-tRNA<sup>fMet</sup>. Subsequently, the large, 50S ribosomal subunit joins the 30S IC, the IFs dissociate and the resulting 70S IC enters the translation elongation stage. Figure reproduced, with permission, from Wang *et al.*<sup>42</sup>.

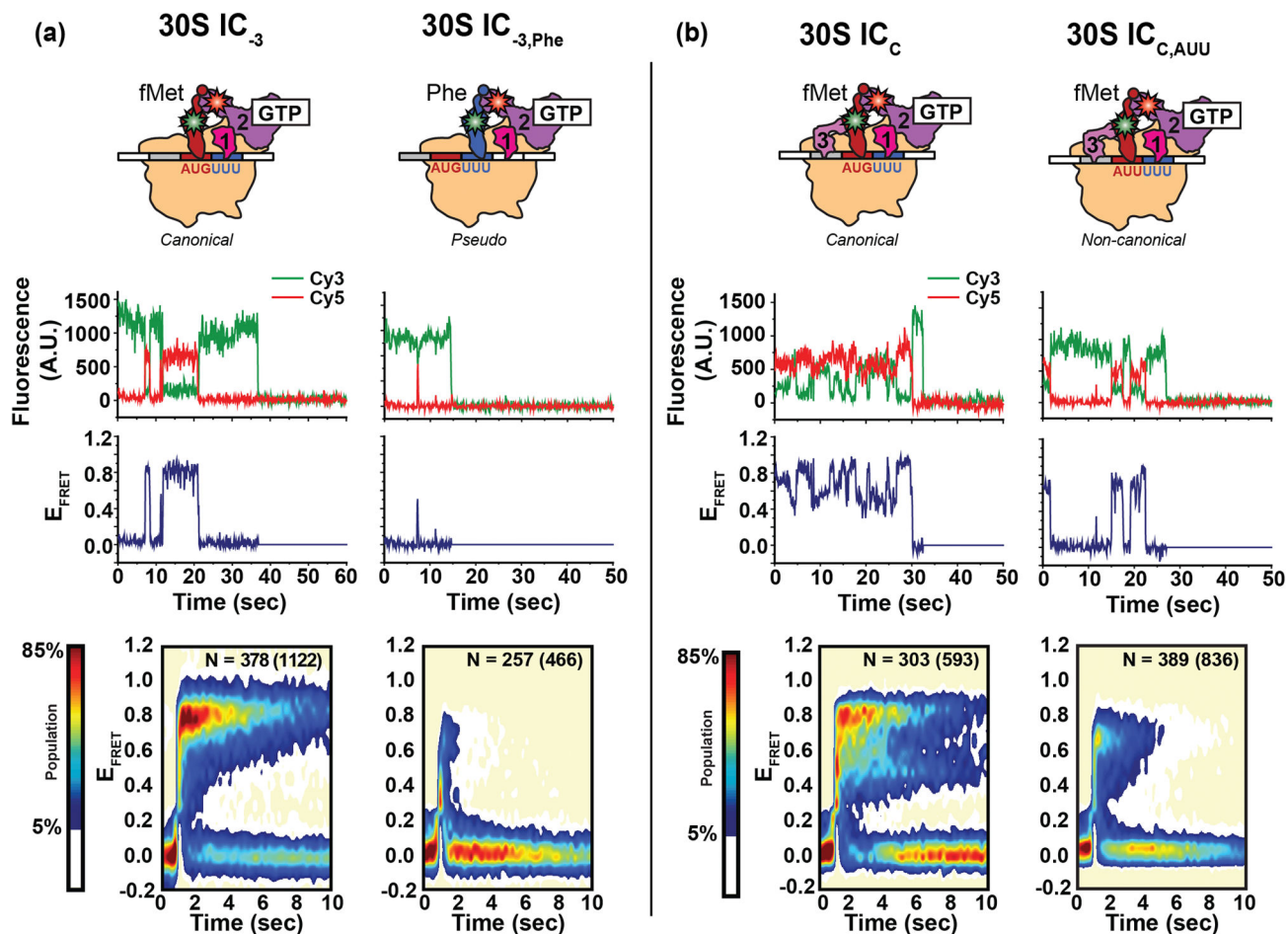


**Figure 2.**

Single-molecule FRET measurements of the IF2•tRNA sub-complex on the 30S IC. (a) Comparison of a canonical 30S IC lacking IF3 (left panel) carrying fMet-tRNA<sup>fMet</sup> base paired to the AUG start codon and the analogous pseudo 30S IC carrying the elongator Phe-tRNA<sup>Phe</sup> (right panel). (b) Comparison of a completely assembled canonical 30S IC (left panel) and the analogous non-canonical 30S IC formed on the near-start AUU codon (right panel). Cartoon representations of the 30S ICs (top row), representative fluorescence versus time trajectories and the corresponding FRET efficiency (E<sub>FRET</sub>) versus time trajectories (middle row), and post-synchronized surface contour plots of the time evolution of population FRET (bottom row) are shown for each 30S IC. Surface contour plots were constructed by superimposing all of the individual IF2 binding events. 'N' values indicate the total number of EFRET versus time trajectories obtained for each 30S IC; the number in parenthesis indicates the total number of IF2 binding events for all of the trajectories (N). Surface contour plots were plotted from the lowest (tan) to the highest (red) population as indicated in the population color bar. Figure adapted, with permission, from Wang *et al.*<sup>42</sup>.

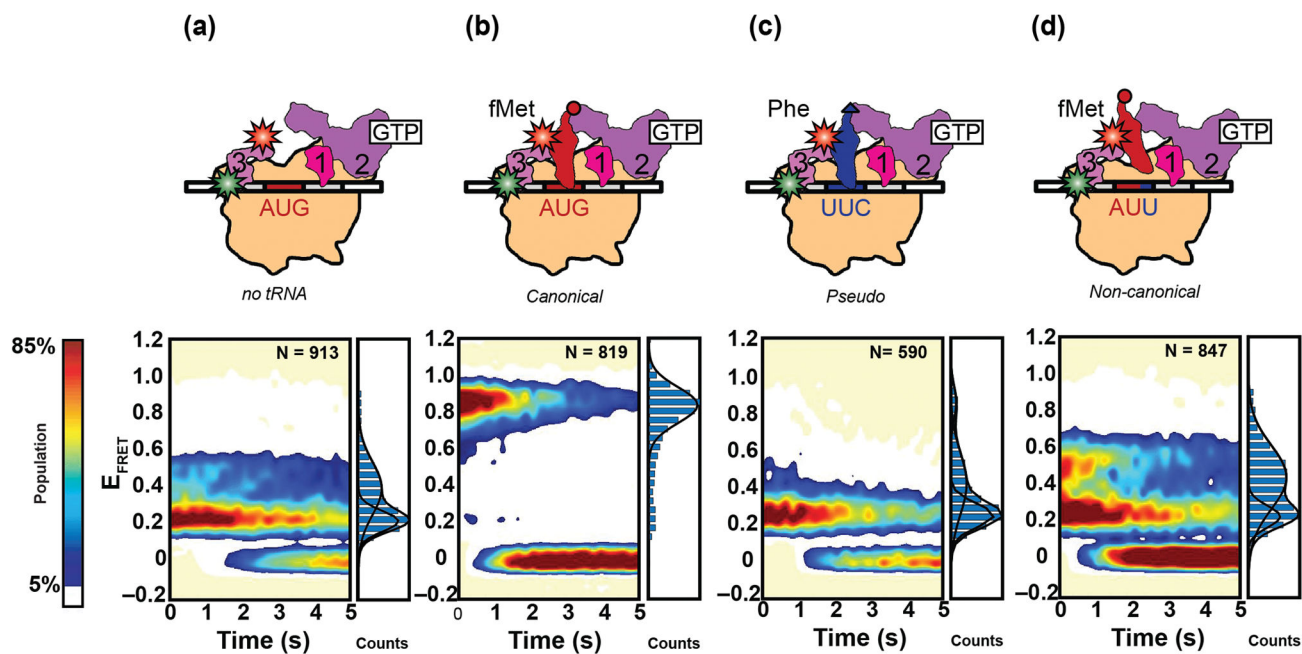


**Figure 3.**

Single-molecule FRET measurements of 30S-bound IF3. Cartoon representations (top row) of various 30S ICs including (a) a 30S IC lacking a tRNA, (b) a canonical 30S IC carrying fMet-tRNA<sup>fMet</sup> base paired to the AUG start codon, (c) a pseudo 30S IC carrying Phe-tRNA<sup>Phe</sup>, and (d) a non-canonical 30S IC assembled on the AUU near-start codon. Surface contour plots (bottom row) of the time-evolution of population FRET were constructed for each 30S IC by superimposing all of the individual EFRET versus time trajectories obtained (not shown), which is given by the ‘N’ value. Normalized one-dimensional EFRET histograms are shown to the right of each surface contour plot. Surface contour plots are plotted from the lowest (tan) to the highest population (red) as indicated by the population color bar. Figure adapted from Elvekrog *et al.*<sup>59</sup>.

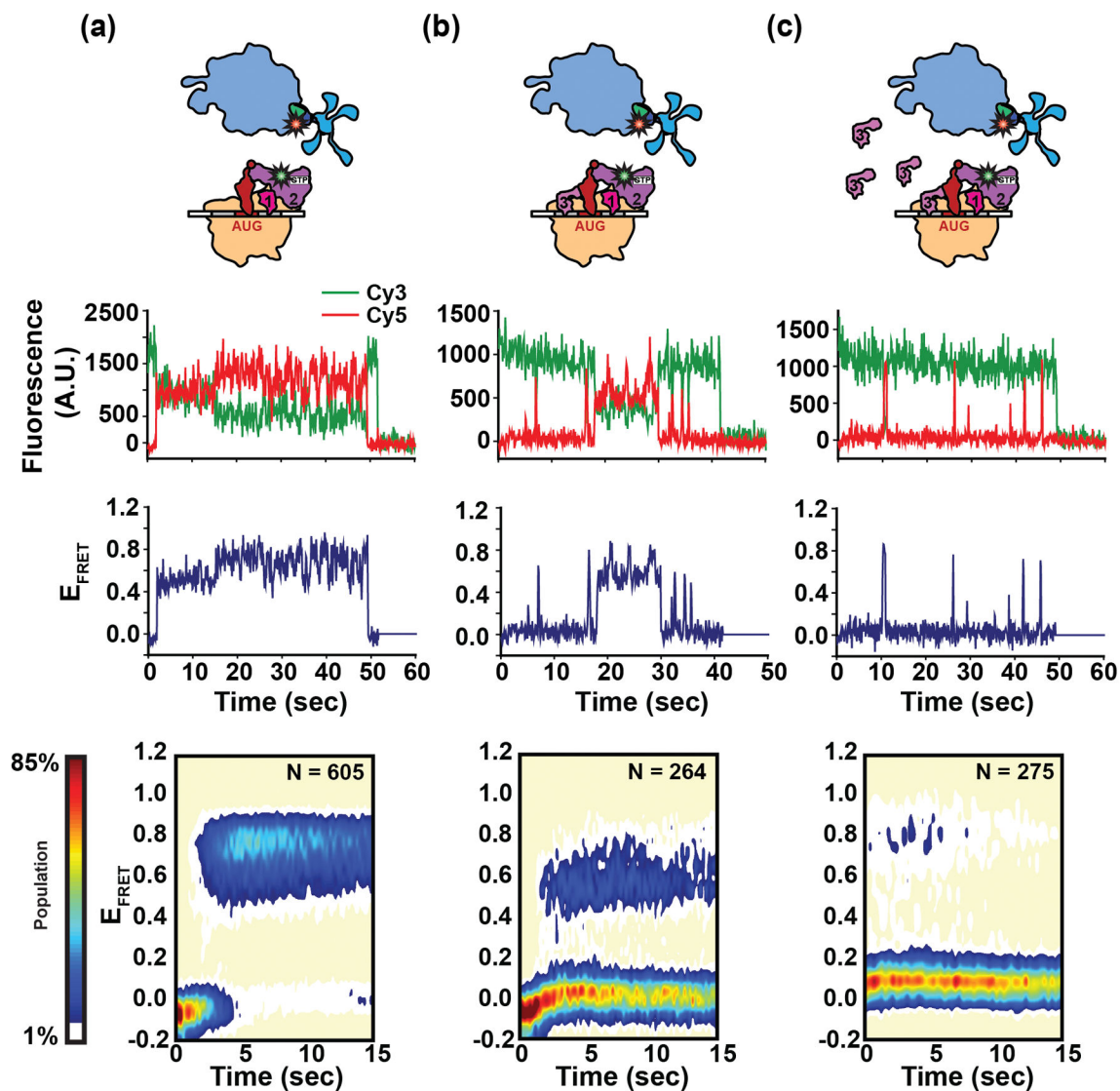


**Figure 4.** Single-molecule measurements of subunit joining. Comparison of the stability and dynamics of subunit joining to IF2-bound 30S ICs formed in (a) the absence of IF3, (b) a ~1:1 ratio of IF3 to 30S ribosomes and (c) in the presence of excess free IF3 in solution. Cartoon representations (top row), representative fluorescence versus time, and the corresponding EFRET versus time trajectories (middle row), and surface contour plots of the time evolution of population FRET (bottom row) are shown for each 30S IC. The number of EFRET versus time trajectories that were superimposed to construct the surface contour plot is given by 'N'. Surface contours were plotted from the lowest population (tan) to the highest population (red) as indicated by the population color bar. Figure adapted, with permission, from Macdougall *et al.*<sup>60</sup>.